Title
Results from the AMANDA experiment

Permalink
https://escholarship.org/uc/item/4sc4h4jb

Journal
Modern Physics Letters A, 22(24)

ISSN
0217-7323

Author
Silvestri, Andrea

Publication Date
2007-08-01

Peer reviewed

Results from the AMANDA Experiment

ANDREA SILVESTRI[†] for the IceCube Collaboration[*]

*Department of Physics and Astronomy, University of California
Irvine, CA 92697, U.S.A.
[†]E-mail: silvestr@uci.edu*

The Antarctic Muon And Neutrino Detector Array (AMANDA) has been taking data
since 2000 and its data acquisition system was upgraded in January 2003 to read out the
complete digitized waveforms from the buried Photomultipliers (PMTs) using Transient
Waveform Recorders (TWR). This system currently runs in parallel with the standard
AMANDA data acquisition system. Once AMANDA is incorporated into the 1 km^3
detector IceCube, only the TWR system will be kept. We report results from a first
atmospheric neutrino analysis on data collected in 2003 with TWR. Good agreement in
event rate and angular distribution verify the performance of the TWR system. A search
of the northern hemisphere for localized event clusters shows no statistically significant
excess, thus a flux limit is calculated, which is in full agreement with previous results
based on the standard AMANDA data acquisition system. We also update the status
of a search for diffusely distributed neutrinos with ultra high energy (UHE) using data
collected by the TWR system.

Keywords: Neutrino Detector; Neutrino Astronomy; Point Sources; Diffuse Sources; Ultra
High Energy Neutrinos.

PACS Nos.: include PACS Nos.

Introduction

Neutrinos are the only high energy particles able to propagate undeflected and
unattenuated from the furthest reaches of the Universe. Extragalactic UHE γ-ray
astronomy falters for energies greater than a few tens of TeV due to interactions
with infrared and Cosmic Microwave Background photons. The information carried
by the neutrino messengers from distant, unexplored regions of the universe may
help to unravel longstanding mysteries associated with the origin of the highest
energy cosmic rays. Several models[1,2,3,4,5,6] predict high energy charged particle and
neutrino emission; the diffuse ν-flux predictions by these models are constrained by
the observed cosmic ray fluxes[7]. AMANDA[8], the first neutrino telescope constructed
in transparent ice, is deployed between 1500 m and 2000 m beneath the surface at

---

[*]http://www.icecube.wisc.edu

the geographic South Pole. It is designed to search for neutrinos that originate in the most violent phenomena in the observable universe. Galactic objects like Supernova Remnants (SNR) and extragalactic objects such as Active Galactic Nuclei (AGN) are expected to be the powerful engines accelerating protons and nuclei to the highest energies, which eventually interact to generate neutrinos. We have searched for point sources in the northern sky and for a diffuse flux of UHE ($E_\nu > 10^{15}$ eV) neutrinos of cosmic origin. We have performed the analysis using data collected in 2003 with a new data acquisition system based on Transient Waveform Recorders (`TWR-DAQ`), which we compared to data collected by the standard AMANDA readout system (μ-`DAQ`).
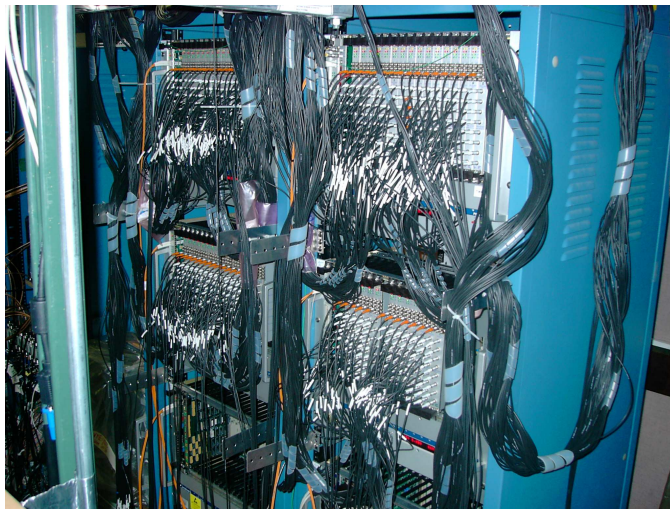

Fig. 1.   The upgraded AMANDA data acquisition electronics with Transient Waveform Recorders, here displayed in a system of 2 racks with 72 TWR modules.

1. The TWR System

The data acquisition electronics of the AMANDA-II detector (Fig. 1) was upgraded in 2003 to read out the complete digitized waveform of the photomultiplier tubes (PMTs) using Transient Waveform Recorders (TWR)[9]. The transition was made to run the μ-`DAQ`[10] and `TWR-DAQ` in parallel to verify that the performance of the latter is as good or better. To compare the two systems, the data from 2003 has been analyzed with data sets from both readout systems. The performance of the `TWR-DAQ` is verified by comparing the results for the absolute rate of atmospheric neutrinos and the $cos(\theta)$ distribution with the results from the standard μ-`DAQ`[11]. Extending the analysis tools to include `TWR` data required several new developments: (1) The `TWR-DAQ` measures the integrated charge $\mathcal{Q}$ from the full waveform of the

PMT pulses, in contrast, the μ-DAQ only measures the maximum amplitude of the PMT pulse in a 2 μs window. (2) Various time offsets were taken into account for the TWR-system, none of which impacted the μ-DAQ. A time resolution of few nanoseconds was extracted. (3) The size of the TWR-DAQ data set (20TB for 2003) by far exceeds that of the μ-DAQ ($\sim$1TB), requiring an improved data handling tools.

2. Analysis

The data information of the two systems has been merged according to GPS time and the fraction of overlapping PMTs participating in the event in both systems. For the point source analysis we restricted the capabilities of the TWR-DAQ system to mimic the features of the μ-DAQ system as closely as possible. The timing and amplitude information extracted from waveforms has been used as input parameters to perform PMT-pulse cleaning, TOT (Time-Over-Threshold) and crosstalk[a] cleaning. A Gaussian fit of the distribution for $\Delta t = t_\mu - t_{TWR}$ yields $\sigma_{\Delta t} = 4.2$ ns
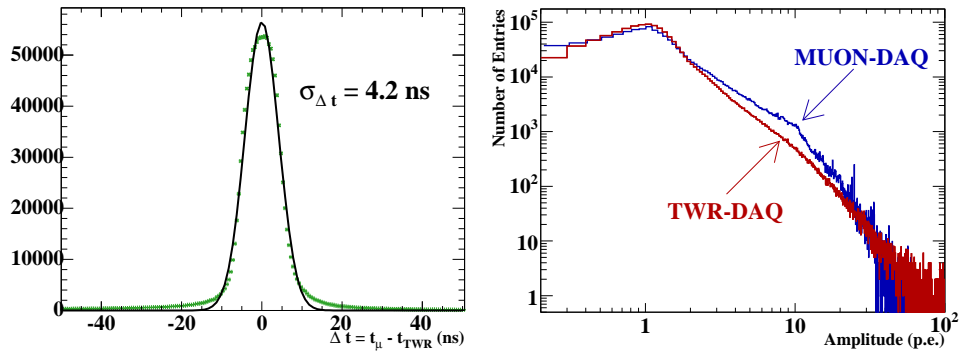

Fig. 2.   (Left) Time difference between the PMT pulses recorded by the two acquisition systems $\Delta t = t_\mu - t_{TWR}$. (Right) Calibrated amplitude normalized to 1 photo-electron (p.e.) value for μ-DAQ and TWR-DAQ data. See text for details.

(Fig. 2 (left)), which is dominated by the systematic error of the time jitter between independent flash ADC clocks of the TWR system. The TWR-DAQ timing calculations are relative to the values measured by the μ-DAQ. The timing of the TWR-DAQ system includes two sources of jitter, the digitization window of 10 ns and the time fluctuation of the flash ADC clocks within the same 10 ns interval. This accounts for the $\sigma_{\Delta t} \sim 4$ ns[b]. Amplitudes are also calibrated by extracting the number of photo-electrons (Npe) detected from the peak ADC of the μ-DAQ and charge $\mathcal{Q}$ of the TWR system and normalized to 1-pe amplitude. By integrating the charge

---

[a]Any phenomenon by which a signal transmitted on one channel of a transmission system creates an undesired effect in another channel.
[b]For year 2005 the phases of the TWR modules were synchronized to avoid the time jitter between independent flash ADC clocks.

4 *Andrea Silvestri et al.*

Table 1.   Passing rates for increasing level of data selection criteria for the `TWR-DAQ` and μ-`DAQ` data analysis.

Selection	`TWR-DAQ`	μ-`DAQ`
Level-0 (Raw)	1.86×10^9	1.86×10^9
Level-1	1.25×10^8	1.25×10^8
Level-2	2.56×10^6	1.99×10^6
Level-3 (Final)	1112	1026

from pulses in the waveform, the dynamic range of the `TWR-DAQ` extends to Npe of ~ 100, a factor of three higher than the μ-`DAQ`. Fig. 2 (right) shows the reconstructed amplitude of the `TWR-DAQ` compared to the μ-`DAQ`, which indicates a stable power law distribution extending up to 100 Npe, while the μ-`DAQ` system shows a "knee" around 10 Npe. The knee is due to the amplitude saturation of channels read out by optical fibers, which comprise $\sim$40% of the AMANDA channels.[c] After cleaning, the muon track is reconstructed from the pulse times of the PMTs. Details on the reconstruction techniques can be found in[12]. Table 1 summarizes the passing rates from the raw data level to the final sample of atmospheric neutrinos. The event selection criteria used in this analysis follows the method described in[13]. Fig. 3 shows that the angular mismatch for the final neutrino sample $\sigma_{\Delta\theta}$ is $0.5°$ where $\Delta\theta = \theta_\mu - \theta_{TWR}$. This value is expected from studies of the precision of the global minimizer in the reconstruction program, by reconstructing the same event sample twice with a 32-iteration algorithm. The azimuth angular mismatch $\sigma_{\Delta\phi}$ is $0.7°$, which is consistent with a σ of $0.5°$ for the $\Delta\phi \times \sin(\theta)$ distribution to account for the zenith dependence on the azimuth angle.
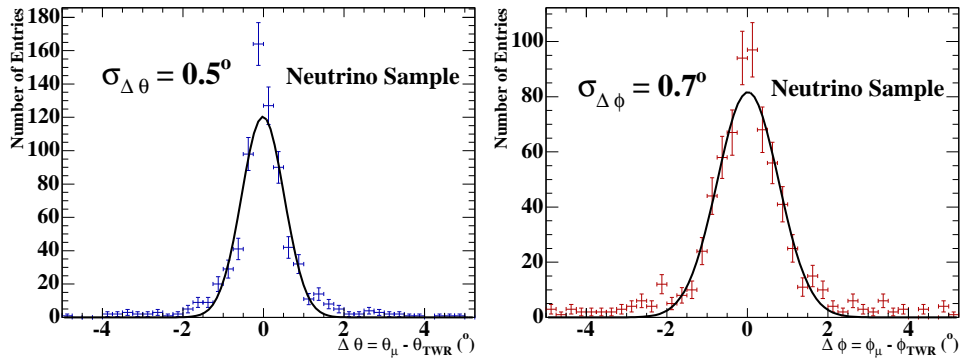

Fig. 3.   (Left) The zenith $\Delta\theta = \theta_\mu - \theta_{TWR}$ difference distribution between the μ-`DAQ` and the `TWR-DAQ` systems, (right) the azimuthal $\Delta\phi = \phi_\mu - \phi_{TWR}$ difference distribution.

[c]High voltage values were lowered in January 2005 to increase linear dynamic range of optical channels.

3. Search for Point Sources of Neutrinos

From the analysis based on `TWR-DAQ` data, 1112 neutrinos are observed compared to 1026 neutrinos from the μ-`DAQ` data analysis. The small differences in the event rate are compatible with the small differences in analysis procedures described in Section 2. Fig. 4 shows the $\cos(\theta)$ distribution of the atmospheric neutrino sample
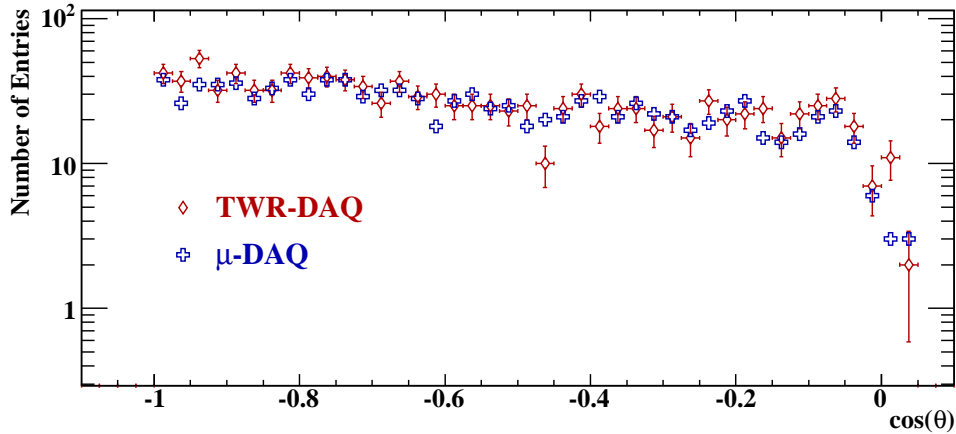

Fig. 4.   Distribution of $\cos(\theta)$ after final selection representing the atmospheric neutrino sample observed from the `TWR-DAQ` and the μ-`DAQ` analyses.

extracted from the `TWR-DAQ` and μ-`DAQ` data analysis. Satisfactory agreement can be seen for the $\cos(\theta)$ distribution of the atmospheric neutrinos samples obtained by the different analyses. Fig. 5 displays the sky map plotted in equatorial coordinates of the 1112 atmospheric neutrino candidates observed from the `TWR-DAQ` analysis. All events are distributed in the norther hemisphere with very few events reconstructed at the horizon. In order to distinguish if the observed events follow a random distribution as expected by atmospheric neutrinos, or are an indication of localized event cluster as expected by a source of neutrinos of extraterrestrial origin, an analysis is required to estimate the statistical significance of the observed events. A full search of the northern sky was performed to look for any localized event cluster. The full scan is extended to 85° in declination, since the limited statistics in the polar bin prevents an accurate estimate of the background. Fig. 6 shows the sky map of the calculated significance for all observed 1112 events in terms of the a positive or negative deviation with respect to the mean background events. All observed regions with the highest significance are compatible with the background hypothesis. The highest significance observed shows a positive deviation of 4.3 σ, which corresponds to a probability of 23% for a search performed on events with randomized right ascension. Numerous studies have been performed to implement the best possible description of the TWR system in the Monte Carlo
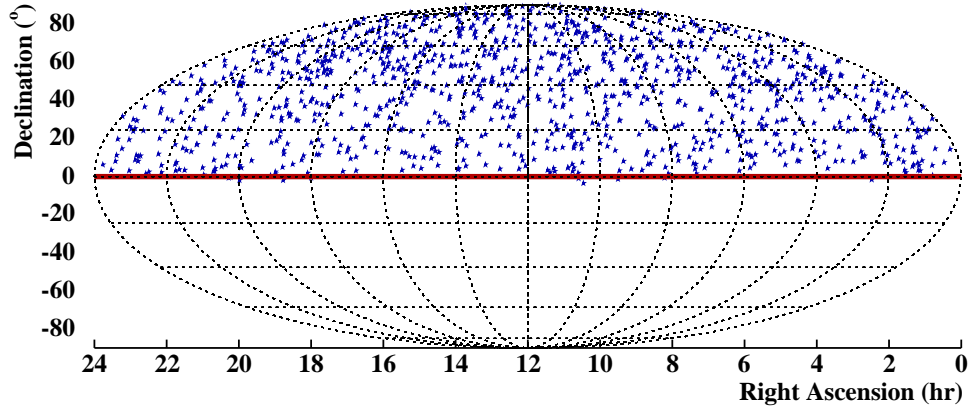
6   *Andrea Silvestri et al.*

Fig. 5.   Sky plot displayed in equatorial coordinates, Right Ascension (RA) and Declination (DEC), of the final sample of 1112 atmospheric neutrinos observed from the `TWR-DAQ` analysis.

simulation. In particular, a correct description of the waveform hardware response is now available and proper TDC time windows as well as amplitude calculations have been now implemented. Therefore a calculation of the neutrino effective area for point source search using TWR data is now feasible. Fig. 7 (left) shows the effective muon neutrino area as a function of E_{ν_μ} computed at the final selection of this analysis for four separated ranges of the declination. The A^ν_{eff} extends over six order of magnitudes as ν-energy increases, while A^ν_{eff} decreases as declination increases due to the neutrino absorption in the Earth. The average upper limit on ν_μ as a function of declination is shown in the right panel of Fig. 7. The average neutrino flux upper limit is determined from the ratio of the average Feldman and Cousins[14] upper limit $< \mu^{90} >$ computed according to the expected mean background and observed events, and the number of the expected signal events for a neutrino flux $E^2_\nu d\Phi_\nu/dE_\nu = $ GeV s^{-1}cm^{-2} from a point source at declination δ.
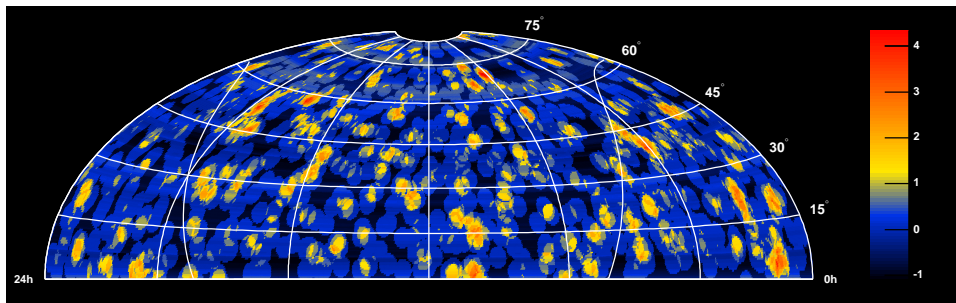

Fig. 6.   Sky map plotted in coordinates of right ascension and declination of the 1112 atmospheric neutrino candidates from the `TWR-DAQ` analysis. The scale on the right reflects excess or deficit in terms of the positive or negative deviation with respect to the mean background events.

Together with the average upper limit extracted from the `TWR-DAQ` data, the limit from the μ-`DAQ` data of year 2003[13] is also represented for comparison. These results are comparable, however the `TWR-DAQ` limit is $\sim 10\%$ worse than the μ-`DAQ` limit, because conservative event selection criteria have been applied that do not use the full waveform information in an optimal way. The preliminary average upper limit from the `TWR-DAQ` analysis on the muon neutrino flux with spectrum $\mathrm{d}\Phi_\nu/\mathrm{d}E_\nu \propto E_\nu^{-2}$ is $E_\nu^2 \mathrm{d}\Phi_\nu/\mathrm{d}E_\nu \leq 1.8 \times 10^{-7}$ GeV s^{-1}cm^{-2} at 90% confidence level, in the energy range 1.26 TeV $< E_\nu < 1.6$ PeV. This upper limit does not include systematic uncertainties. AMANDA has submitted a publication on a 5-year search for point sources (2000-2004) based on the μ-`DAQ` data[13], which improves the limit by $\sim 67\%$ compared to the results from this analysis.
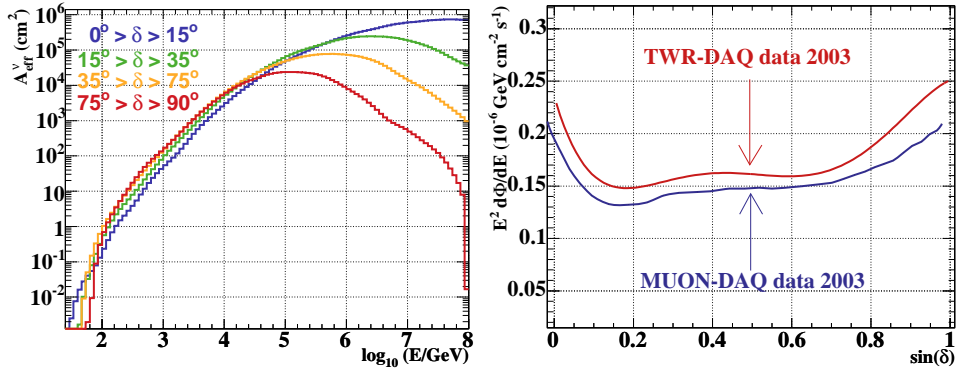

Fig. 7.   (Left) Muon neutrino effective area as a function of E_{ν_μ} for point source searches displayed for different declinations δ. (Right) Average upper limit as a function of $\sin(\delta)$ on ν_μ for a E^{-2} neutrino flux spectrum from the `TWR-DAQ` and the μ-`DAQ` analyses.

4. Search for UHE Neutrinos

The search for UHE neutrinos differs from the point source mainly in two aspects. First, the search for point sources is restricted to upward going events of energy within the TeV scale, the UHE analysis extends the search beyond PeV energies. Second, while point sources are localized in a small region of the sky, UHE diffuse neutrinos are expected to come from the entire visible sky (2π sr), with a higher probability to originate from the horizon. Fig. 8 shows one of the 1112 upward going neutrino events and an almost horizontal UHE simulated neutrino event with energy $E \sim 3 \times 10^{15}$ eV. Simulated events with energy above one PeV deposit a substantial amount of light which is recorded by almost all PMTs. In order to better separate background events from signal events, we developed new variables which exploit the information of the full waveforms. The capability of improved photo-electron reconstruction of the `TWR-DAQ` system can be seen in Fig. 9, which displays a contour plot in $\log_{10}$-scale of the sum of the reconstructed number of
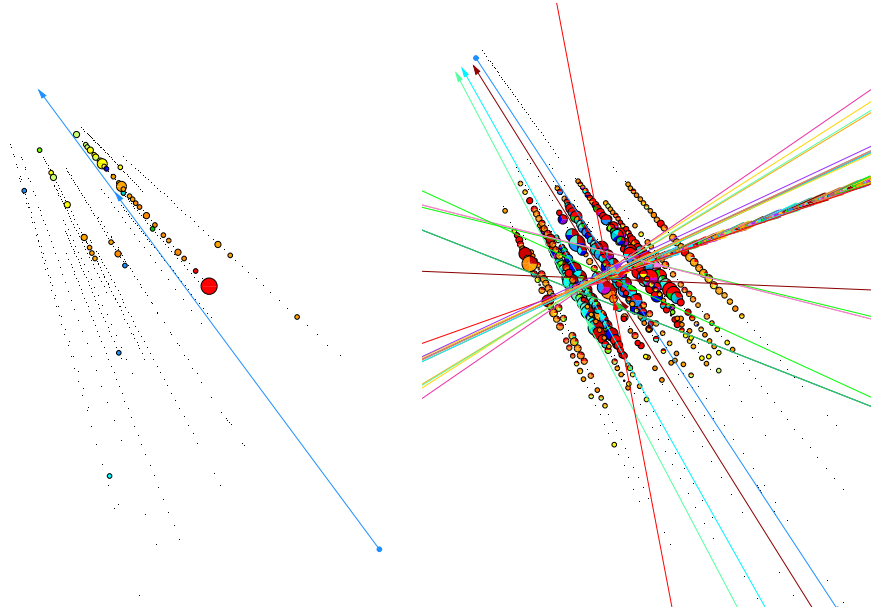
8   *Andrea Silvestri et al.*

Fig. 8.   (Left) one of the 1112 atmospheric neutrino event detected in the experimental array. (Right) a high-energy MC simulated event. The size of the circles represent energy deposited in the detector, the colors represent the time profile of photons propagating in the ice which have scattered to the PMTs.

PE, NPE_{reco} versus the NPE_{true} generated by the signal MC simulation. While the μ-DAQ system quickly saturates on the order of few thousands of PE's, the TWR-DAQ, by using the after-pulse information, can see the millions of PE's which are typical for UHE events triggered by single muons. Fig. 10 summarizes the results
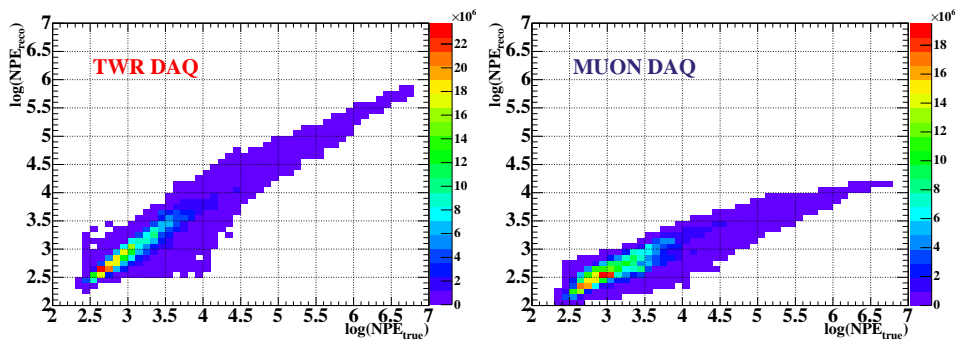

Fig. 9.   Contour plots displaying the capability of correctly reconstructing the total number of photon-electron injected into the detector (left) for the TWR-DAQ and (right) for the μ-DAQ system.

of several AMANDA searches for diffuse neutrinos at different energy ranges using μ-DAQ data. The experimental limits assume a 1:1:1 ratio of neutrino flavors at the Earth due to oscillation. The dotted and dashed lines represent a sample of model predictions[1,2,3,4,6], adjusted for oscillation if necessary. The horizontal solid lines represent limits on the integrated neutrino flux from the diffuse analyses with AMANDA-B10[15], with AMANDA-II[16], from the cascade analysis[17], and from the UHE analysis[18,19], with the NT200 neutrino telescope[20], and at the highest energies from ANITA-lite[21] and RICE[22]. These are the most stringent flux limits at 90% C.L. for an E^{-2} spectrum to date. The AMANDA limits have been determined by analysing data collected with the μ-DAQ system. However, as it has been shown above, by performing a new analysis approach with TWR-DAQ data, it is possible to develop new techniques and to improve the current experimental limits for the UHE neutrino search.
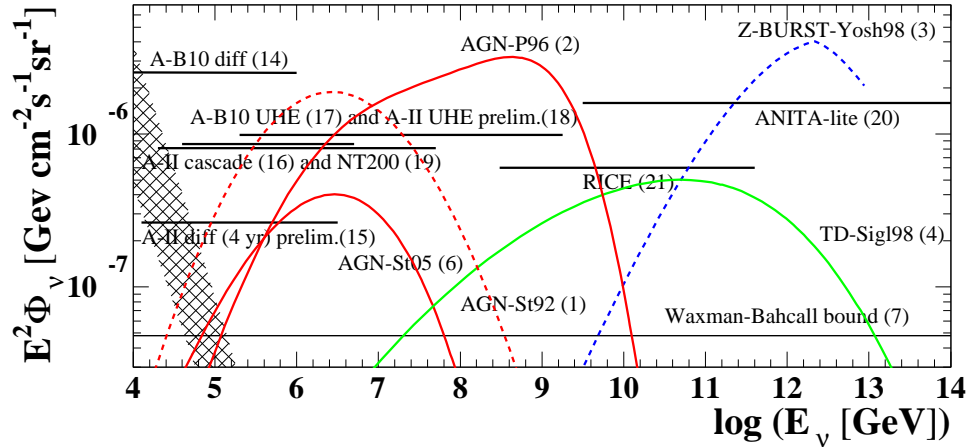

Fig. 10. Experimental limits on the integrated neutrino flux and detector sensitivity for a neutrino flux of E^{-2} spectrum. The curves represents predictions from theoretical models, the solid lines show current AMANDA (all-flavor limits), NT200, ANITA and RICE experimental limits.

5. Conclusion

The point source search provides the first detailed evaluation of the performance of the TWR-DAQ system. This analysis demonstrated that the TWR-DAQ produces similar event rates and angular distribution as the data collected by the standard μ-DAQ system. No statistically significant excess has been observed after performing a full search of the northern hemisphere of the sky for localized event clusters, therefore a flux limit based on TWR-DAQ data is calculated. The AMANDA TWR readout is now being incorporated into the IceCube data acquisition system. By exploiting the information of the full waveforms from the TWR-DAQ system, it is possible to

develop new analysis techniques for an improved search for diffuse UHE neutrinos. Currently the AMANDA experiment has placed the most stringent neutrino flux limits to date, which can be further improved by analyses performed with `TWR-DAQ` data.

Acknowledgments

References

1. F. Stecker et al., *Phys. Rev. Lett.* **66**, 2697 (1992).
2. R. J. Protheroe, *astro-ph/9607165* (1996).
3. S. Yoshida et al., *Phys. Rev. Lett.* **81**, 5505-5508 (1998).
4. G. Sigl, *Phys. Rev. D* **59**, 043504 (1999).
5. R. Engel et al., *Phys. Rev. D* **64**, 093010 (2001).
6. F. W. Stecker, *Phys. Rev. D* **72**, 107301 (2005).
7. E. Waxman and J. Bahcall, *Phys. Rev. D* **59**, 023002 (1999).
8. A. Silvestri et al., in *Neutrinos and Explosive Events in the Universe*, Springer, New-York, **209**, 275-285 (2005).
9. W. Wagner et al., in *28th ICRC*, **2**, 1365-1368 (2003).
10. R. Wischnewski et al., in *27th ICRC*, **2**, 1105-1108 (2001).
11. A. Silvestri et al., in *29th ICRC*, **5**, 431-434 (2005).
12. J. Ahrens et al., *Nucl. Instrum. Meth.* **A524**, 169 (2004).
13. A. Achterberg et al., *astro-ph/0611063* (2006).
14. G. J. Feldman and R. D. Cousins, *Phys. Rev. D* **57**, 3873 (1998).
15. J. Ahrens et al., *Phys. Rev. Lett.* **90**, 251101 (2003).
16. G. Hill et al., in Proc. of the XXII International Conference on Neutrino Physics and Astrophysics (2006).
17. M. Ackermann et al., *Astropart. Phys.* **22**, 127 (2005).
18. M. Ackermann et al., *Astropart. Phys.* **22**, 339 (2005).
19. L. Gerhardt et al., in Proc. of SUSY06 (2006).
20. V. Aynutdinov et al., *Astropart. Phys.* **25**, 140 (2006).
21. S. Barwick et al., *Phys. Rev. Lett.* **96**, 171101 (2006).
22. I. Kravchenko et al., *Phys. Rev. D* **73**, 082002 (2006).